DOI: 10.1021/ic101189w

Inorganic Chemistry
Article

# Thermodynamical and Structural Study of Protactinium(V) Oxalate Complexes in Solution

**Mickaël Mendes,*[,†] Séna Hamadi,[†,‡] Claire Le Naour,*[,†,‡] Jérôme Roques,[†,‡] Aurélie Jeanson,[†,‡] Christophe Den Auwer,[§] Philippe Moisy,[§] Sylvain Topin,[∥] Jean Aupiais,[∥] Christoph Hennig,[⊥] and Maria-Vita Di Giandomenico[‡,⊗]**

[†]*Université Paris-Sud, Institut de Physique Nucléaire, UMR 8608 Orsay, F-91406, France,* [‡]*CNRS/IN2P3, Orsay, F-91406, France,* [§]*CEA, Nuclear Energy Division, RadioChemistry and Process Department, F-30207 Bagnols sur Cèze, France,* [∥]*CEA, DAM, DIF F-91297 Arpajon, France,* [⊥]*Forschungszentrum Dresden-Rossendorf, Institute of Radiochemistry, D-01314 Dresden, Germany, and* [⊗]*EDF R&D MMC, Site des Renardières, F-77818 Moret sur Loing, France*

Received June 14, 2010

The complexation of protactinium(V) by oxalate was studied by X-ray absorption spectroscopy (XAS), density functional theory (DFT) calculations, capillary electrophoresis coupled with inductively coupled plasma mass spectrometry (CE-ICP-MS) and solvent extraction. XAS measurements showed unambiguously the presence of a short single oxo-bond, and the deduced structure agrees with theoretical calculations. CE-ICP-MS results indicated the formation of a highly charged anionic complex. The formation constants of $PaO(C_2O_4)^+$, $PaO(C_2O_4)_2^-$, and $PaO(C_2O_4)_3^{3-}$ were determined from solvent extraction data by using protactinium at tracer scale ($C_{Pa} < 10^{-10}$ M). Complexation reactions of Pa(V) with oxalate were found to be exothermic with relatively high positive entropic variation.

## Introduction

Protactinium ($Z = 91$) occupies a key position between thorium and uranium as the first actinide with 5*f* electrons or vacant 5*f* orbitals involved in bonding. In solution and in solid state, the most stable oxidation state of protactinium is 5+ which corresponds to the electronic configuration $5f^0$. Unlike other light actinides at oxidation states 5+ and 6+ that form a linear transdioxo moiety, protactinium complexes are characterized by at most one mono oxo bond.[1−5] The occurrence or absence of this mono oxo bond depends on the media: the species $PaF_7^{2-}$ and $PaO(SO_4)_3^{3-}$ have been observed in hydrofluoric acid and high concentrated sulfuric acid, respectively.[1−4] The main feature in protactinium chemistry is a strong tendency toward hydrolysis leading to sorption on any solid support material.[1,2,5] Moreover, at high protactinium concentration an irreversible polymerization occurs, which restricts experiments that can be performed with this element. Polymerization of Pa(V) has been observed even in concentrated HCl or 4 M $H_2SO_4$. This problem can be overcome only by use of strong ligands like fluoride or by using tracer scale Pa concentrations.[2−4] Therefore, thermodynamic data related with Pa chemistry in aqueous solution are rather scarce, and the most reliable ones have been determined with the element at very low concentration ($C_{Pa} < 10^{-10}$ M).[2,5] With the aim to improve the knowledge on the physicochemical properties of light actinides, studies on Pa are conducted according to a dual approach: a structural one with Pa in macro amount and a thermodynamic one with Pa at tracer scale. Besides, isotopes $^{233}$Pa ($\beta^-$ emitter, $T_{1/2} = 27$ d) and $^{231}$Pa ($\alpha$ emitter, $T_{1/2} = 32700$ y) will be produced in thorium fuel reactors that are under consideration for long-term energy production. Protactinium must therefore be taken into account in the waste management: safety prediction for the disposal of radioactive waste containing Pa requires structural and thermodynamic data necessary for modeling its behavior in the environment.

In the present work, oxalic acid was chosen since it is expected to behave as a strong ligand toward Pa(V). Moreover oxalic acid, produced by fungi or exsuded by roots of plants, may be initially present in groundwater or may form in course of radiation damage of more complex polycarboxylic acids.[6,7] Literature devoted to the behavior of protactinium in presence of oxalate is rather scarce and controversial. Ion exchange

*To whom correspondence should be addressed. E-mail: lenaour@ipno.in2p3.fr (C.L.N.), mickael.mendes@free.fr (M.M.). Fax: 33 1 69 15 71 50.

(1) Brown, D.; Maddock, A. G. Analytical Chemistry. In *Progress in Nuclear Energy*; Pergamon press: Oxford & New York, 1967; p 8-1.
(2) Muxart, R.; Guillaumont, R. Protactinium. In *Compléments au Nouveau Traité de Chimie minérale*; Masson: Paris, 1974.
(3) Di Giandomenico, M. V. Ph.D. Thesis, Université Paris Sud, Orsay, France, 2007; available at http://hal.archives-ouvertes.fr/docs/00/26/49/52/PDF/these_Vita.pdf.
(4) Le Naour, C.; Trubert, D.; Di Giandomenico, M. V.; Fillaux, C.; Den Auwer, C.; Moisy, P.; Hennig, C. *Inorg. Chem.* **2005**, *44*, 9542.
(5) Myasoedov, B.; Kirby, H. W.; Tananaev, I. G. Protactinium. In *The Chemistry of the Actinide and Transactinide Elements*; Springer: The Netherlands, 2006.
(6) Gammons, C. H.; Wood, S. A. *Chem. Geol.* **2000**, *166*, 103.
(7) Toste, A. P. *J. Radioanal. Nucl. Chem.* **1999**, *239*, 433.


Published on Web 09/30/2010

and solvent extraction experiments, performed at tracer scale, have led to the observation of various oxalate complexes, ranging from (1,1) to (1,4), with or without oxo or/and hydroxo groups.[2,5,8] The corresponding formation constants have been determined but can hardly be compared among each other because of differences in experimental conditions and complexes formulations. A few studies have been performed with protactinium(V) in weighable amount. UV−vis absorption spectra of protactinium(V) in solutions of $H_2C_2O_4$ do not display characteristic absorption peaks, even if an increase in absorption has been noticed with the increase in Pa and oxalic acid concentrations.[2] The precipitation of a white oxalate complex of protactinium was observed at high Pa concentration (0.16 and 0.5 M).[2,5,9] The following species have been proposed: $PaO(OH)C_2O_4,xH_2O$ ($2 \le x \le 4$) and $Pa(OH)(C_2O_4)_2 \cdot 6H_2O$. The X-ray diffraction measurement of the first compound could not be used to determine the structure because of the presence of more than one solid phase. However, in both cases, polymerization of protactinium was deduced from Infrared and total reflectance spectroscopy: the strong absorptions at 500 $cm^{-1}$ and 245 nm respectively have been attributed to the presence of Pa−O−Pa bonds.

In the present work, the study of oxalate complexation of protactinium(V) was conducted at different metal concentration levels. On one hand, the identification of the mean composition of predominant species and their stability constants were deduced from solvent extraction experiments with protactinium at tracer scale. On the other hand, with weighable amount of element, the structure of the maximum order complex was investigated by combining X-ray absorption spectroscopy measurements, density functional theory (DFT) calculations and capillary electrophoresis coupled with inductively coupled plasma mass spectrometry (CE-ICP-MS) to get information on the potential occurrence of a mono oxo bond in this oxalate complex and on its charge.

## Experimental Section

***Caution!*** *$^{231}$Pa is a radioactive isotope and an α-emitter. It must be handled in glovebox to avoid health risks caused by internal contamination.*

**1. Sample Preparation. Isotope 231.** The isotope $^{231}$Pa was taken from a stock available at the Nuclear Physics Institute of Orsay. An equivalent of around 10 MBq of $^{231}$Pa was purified with respect to its daughters ($^{227}$Ac, $^{227}$Th, $^{223}$Ra) by ion-exchange chromatography as described previously.[4] The purification process was followed by γ-spectroscopy.

The purified Pa solution was stored in 1 mL of 1 M HF/8 M HCl. For XAS and CE-ICP-MS measurements, aliquots of this solution were evaporated to dryness in Teflon crucibles, and the residue was taken up in concentrated HCl. This procedure was conducted at least eight times to ensure the elimination of fluoride ions that behave as strong ligand toward Pa(V). Two XAS samples were prepared by taking up the final residue with 300 μL 1 M $H_2C_2O_4$ ($C_{Pa} = 1.24.10^{-2}$ M) on one hand and with the same volume of 0.8 M $H_2C_2O_4$ ($C_{Pa} = 4.95.10^{-3}$ M) on the other hand. The acidity of each sample was calculated assuming that the proton consumption during the dissolution of the residue (protactinium hydroxide), with a ratio ligand/Pa higher than 100, was negligible. This led to a free proton concentration of about 0.2 M in both solutions. For capillary electrophoresis sample, a residue corresponding to 20 Bq was taken up with 500 μL of 0.5 M $H_2C_2O_4$ leading to a concentration of protactinium around $10^{-7}$ M and a free proton concentration of about 0.1 M.

**Isotope 233.** The isotope $^{233}$Pa was produced by neutron irradiation of thorium at the Osiris reactor of CEA Saclay. The whole procedure is described in a previous paper.[3]

**2. CE-ICP-MS Experiments.** A commercial Beckman Coulter P/ACE MDQ capillary electrophoresis system (Fullerton, U.S.A.) equipped with a UV detection mode was used for all the separations. The device is equipped with a tailor-made capillary cartridge support designed for adaptation to an external detector. Conventional fused silica capillaries (Beckman Coulter, Fullerton, U.S.A.) with an internal diameter of 50 μm and lengths of 60 cm were used for the separations. An optical window is located at a distance of 10.2 cm from the capillary inlet. The capillary was maintained at a constant temperature of 25 °C generated by a liquid coolant wrapping the capillary. The capillary outlet is located at 1 mm back to the nose of the nebulizer to ensure the electrical continuity of the circuit. Only a small portion of the capillary, outside the CE apparatus, is not temperature-controlled. New fused silica capillaries were preconditioned prior to use by rinsing with 1 M HCl (Prolabo, Titrinorm), 1 M NaOH (Prolabo, Titrinorm) and deionized water. The capillary was daily rinsed with water and 1 M NaOH prior the experiments.

An Axiom inductively coupled plasma sector field mass spectrometer (ICP-SF-MS; VG Elemental, Winsford, Cheshire, U.K.) was coupled with the capillary electrophoresis. The intrinsic detection limit is about $10^{-16}$ M. In hyphenated mode, the detection limit is close to $10^{-12}$ M. A commercial parallel path micronebulizer (Mira Mist CE, Burgener, Mississauga, Canada) which operates with a makeup liquid (2% $HNO_3$, 10% EtOH, 1 ppb Bi as internal standard) interfaces both apparatuses. Ethanol improves the signal stability by decreasing the superficial tension of water droplets. The makeup liquid is introduced thanks to a syringe pump (11 Pico Plus, Harvard Apparatus, Holliston, Massachusetts, U.S.A.) at a nominal flow rate of 9 μL $min^{-1}$. The nebulizer is connected to a borosilicate spray chamber (Mini glass chamber, Burgener, Mississauga, Canada). The ICP-MS operates in the low resolution mode ($R$ = 362). Bi was used to check the variation of sensitivity during the experiments.

Background electrolytes (BGE) were prepared from weighed amounts of $H_2C_2O_4$ (Aldrich, 99.8%) dissolved in deionized water (Millipore, Alpha-Q, 18.2 MΩ cm) to get a final concentration of 0.5 M $H_2C_2O_4$.

Samples are prepared by mixing Pa(V) stock solution, the BGE, and 0.2 μL of dimethylformamide (DMF; BDH, AnalaR ≥ 99.5%). The concentration of Pa(V) in the sample is about $10^{-7}$ M.

Before each separation, the capillary was washed with BGE during 5 min at 20 psi. Separations were completed within 15 min. Sample injections were hydrodynamically carried out at 1 psi during 5 s. Separations are performed at −3 kV and at a constant pressure of 0.8 psi (to avoid clogging). The voltage value was chosen with respect to the Ohm law. The buffer vial was changed between runs to minimize the effects of the electrolysis.

**3. XAS Data Acquisition and Treatment.** X-ray absorption spectroscopy (XAS) measurements were performed in 200 μL cells specifically designed for radioactive samples. XAS measurements of protactinium were carried out on the Rossendorf beamline (ROBL) at ESRF (6.0 GeV at 200 mA) in fluorescence mode, at room temperature, with a Si(111) water cooled monochromator in a channel cut mode. Two Pt coated mirrors were used for harmonic rejection. Energy calibration was carried out with a Y foil (17052 eV at the absorption maximum). All spectra were acquired at the Pa $L_{III}$ edge (16733 eV). Data treatment was performed with the Athena code.[10] Signal noise in $k$-space, $\varepsilon$,

(8) Guillaumont, R. Ph.D. Thesis, Université de Paris, Paris, France, 1966.
(9) Muxart, R.; Guillaumont, R.; Vernois, J. *C. R. Acad. Sci. Paris* **1966**, *262*, 888.
(10) Ravel, B.; Newville, M. *J. Synch. Rad.* **2005**, *12*, 537.

was calculated with the Cherokee code.[11] Data fitting was carried out with the Artemis code[10] in R space between 1.0 and 4.0 Å without prior data filtering (Kaiser window between 2 and 12 $Å^{-1}$). Phases and amplitudes were calculated by using Feff82 and the crystal structure of uranyl oxalate with $Z = 91$ for the absorbing atom.[12,13]

**4. Computational Details.** The $PaO(C_2O_4)_3^{3-}$ structures were optimized using the density functional theory (DFT) approach as implemented in the Gaussian03 package.[14] Calculations were performed using the hybrid B3LYP[15] functional and the PBE0 one which is known to give accurate results for heavy metals.[16,17] Energy-adjusted relativistic effective core potentials (RECPs) developed by Küchle et al.[18] were used (60 core electrons for Pa) with its associated basis set to describe protactinium valence electron density[19] ((14s13p10d8f) contracted in [10s9p5d4f]). A 6-31+G* basis set was used for carbon and oxygen atoms. For both exchange correlation functionals, calculations were performed in vacuum condition and in solution. To take into account part of the solvent effect, the solvation was introduced using a dielectric continuum model of permittivity $\varepsilon_0 = 80$. The conductor-like polarizable continuum model (CPCM) implemented in Gaussian03 was used.[20]

**5. Solvent Extraction Experiments.** Aqueous solutions were prepared by a mixture of three solutions: $NaClO_4$ (Fluka, 99%), $HClO_4$ (Aldrich, 70%), and the complexing agent $H_2C_2O_4$ (Aldrich, 99.8%) dissolved/diluted with deionized water (18.2 MΩ.cm). The organic phase was prepared just prior to use by dissolving the appropriate amount of chelatant 2-thenoyltrifluoroacetone (TTA, Aldrich, 99%) in its hydrate form into toluene (FISHER, 99.99%). Toluene used as diluent was preequilibrated with the corresponding aqueous phase for 3 days.

A total volume of 5 mL composed by 4.95 mL of the previously made aqueous phase and 50 μL of $^{233}$Pa solution (freshly prepared by dilution of the stock solution) was contacted with the same organic phase volume (5 mL) in glass vials. These vials were covered by a film of Galxyl-Parylene (Comelec, Switzerland) to limit the Pa(V) sorption on the glass walls.[21] Extraction experiments were performed at 50 rpm stirring speed in the dark at different temperatures (10, 25, 40, and 50 °C) during sufficient time to achieve distribution equilibrium of TTA as well as Pa(V) between both phases.[21] After separation and 3 mL sampling of each phase, Pa concentration was determined by γ-spectrometry by using the 311.9 keV line of $^{233}$Pa with a germanium detector in a well-defined geometry. The distribution coefficient $D$ of Pa(V) in the system $TTA/toluene/H_2O/NaClO_4/HClO_4/H_2C_2O_4$ was calculated according to eq 1, where $A_{org}$ and $A_{aq}$ refer to the gamma activity of $^{233}$Pa in the organic and aqueous phases respectively.

$$D = \frac{A_{org}}{A_{aq}} \quad (1)$$

Experimental uncertainties have been calculated by taking into account the systematic uncertainties that may occur when preparing the solution as well as random uncertainties associated with gamma activity measurements. It should be noted that any uncertainty associated with the volume lead to uncertainties in free $H^+$ concentration and may have strong influence on $D$ because of acid−base properties of the extractant and the ligand.

Pa(V) sorption on the vessel walls and the related mass balance were determined by comparing the gamma activity of the samples with the activity of three blanks ($A_{blank}$). The blanks were prepared by diluting Pa in 0.2 M HF of the same aliquot as used for the Pa samples. Fluoride is known for its strong complexing ability to Pa avoiding significant sorption on the vessel walls.[1,2,5] The sorption percentage $S$ was estimated using the following equation:

$$S = \frac{A_{blank} - A_{org} - A_{aq}}{A_{blank}} \times 100 \quad (2)$$

In all sets of experiments, the $S$ values were about 10%, whereas proton concentration and ionic strength did not show significant influence.

To quantify the Pa sorbed on the vial walls, 5 mL of 1 M HF was introduced in several vials used for extraction. After 4 h stirring, Pa concentration ($A_{HF}$) in 3 mL sampling was determined by γ-spectrometry. The so obtained sorption percentages ($A_{HF}/A_{blank}$) agree well with that deduced from eq 2, allowing to validate the mass balance and to conclude that no Pa sorption occurred at the vials.

All the thermodynamic data were calculated using the Aqueous Solutions program (version 1.2, 2004).[22]

## Results and Discussion

**1. Structural Study. 1.1. CE-ICP-MS Experiments.** Capillary electrophoresis experiments were performed at CEA of Bruyères-le-Châtel, in a laboratory that is experienced in studies on actinides speciation with this technique.[23] The investigated sample presents a ligand-protactinium ratio equal to $5 \times 10^6$ (with $C^{231}_{Pa} \sim 10^{-7}$ M) corresponding to conditions where the limiting complex is expected. Figure 1 shows the electropherogram registered in anionic mode (voltage −3 kV) for this sample. The line at $8.68 \times 10^5$ ms represents the time delay before the neutral species appears. Observing the oxalate complex of protactinium before that time implies that it is an anionic complex. Moreover, a very negative mobility was observed (two experiments gave electrophoretic mobility of $-3.93$ and $-4.00 \times 10^{-4}$ $cm^2 V^{-1} s^{-1}$, respectively) which is also in good agreement with the behavior of a strong anionic complex. In cationic mode, with a voltage equal to +3 kV (not shown here), the complex was detected after the line associated to DMF, confirming the anionic charge borne by the oxalate complex of Pa(V) of maximum order.

(11) Michalowicz, A. EXAFS code, to be found under http://www.icmpe.cnrs.fr.
(12) Rehr, J. J.; Albers, R. C. *Rev. Mod. Phys.* **2000**, *72*, 621.
(13) Jayadevan, N. C.; Singh Muder, K. D.; Crackraburtty, D. M. *Acta Crystallogr., Sect. B* **1975**, *31*, 2277.
(14) Frisch, M. J.; Trucks, G. W.; Schlegel, H. B.; Scuseria, G. E.; Robb, M. A.; Cheeseman, J. R.; Montgomery, J. A.; Vreven, T.; Kudin, K. N.; Burant, J. C.; Millam, J. M.; Iyengar, S. S.; Tomasi, J.; Barone, V.; Mennucci, B.; Cossi, M.; Scalmani, G.; Rega, N.; Petersson, G. A.; Nakatsuji, H.; Hada, M.; Ehara, M.; Toyota, K.; Fukuda, R.; Hasegawa, J.; Ishida, M.; Nakajima, T.; Honda, Y.; Kitao, O.; Nakai, H.; Klene, M.; Li, X.; Knox, J. E.; Hratchian, H. P.; Cross, J. B.; Bakken, V.; Adamo, C.; Jaramillo, J.; Gomperts, R.; Stratmann, R. E.; Yazyev, O.; Austin, A. J.; Cammi, R.; Pomelli, C.; Ochterski, J. W.; Ayala, P. Y.; Morokuma, K.; Voth, G. A.; Salvador, P.; Dannenberg, J. J.; Zakrzewski, V. G.; Dapprich, S.; Daniels, A. D.; Strain, M. C.; Farkas, O.; Malick, D. K.; Rabuck, A. D.; Raghavachari, K.; Foresman, J. B.; Ortiz, J. V.; Cui, Q.; Baboul, A. G.; Clifford, S.; Cioslowski, J.; Stefanov, B. B.; Liu, G.; Liashenko, A.; Piskorz, P.; Komaromi, I.; Martin, R. L.; Fox, D. J.; Keith, T.; Al-Laham, M. A.; Peng, C. Y.; Nanayakkara, A.; Challacombe, M.; Gill, P. M. W.; Johnson, B.; Chen, W.; Wong, M. W.; Gonzalez, C.; Pople, J. A.; *Gaussian 03*, Revision C.02; Gaussian, Inc.: Wallingford, CT, 2004.
(15) Becke, A. D. *J. Chem. Phys.* **1993**, *98*, 5648.
(16) Vetere, V.; Adamo, C.; Maldivi, P. *Chem. Phys. Lett.* **2000**, *325*, 99.
(17) Di Giandomenico, M. V.; Le Naour, C.; Simoni, E.; Guillaumont, D.; Moisy, P.; Hennig, C.; Conradson, S. D.; Den Auwer, C. *Radiochim. Acta* **2009**, *97*, 347.
(18) Küchle, W.; Dolg, M.; Stoll, H.; Preuss, H. *J. Chem. Phys.* **1994**, *100*, 7535.
(19) Cao, X.; Dolg, M.; Stoll, H. *J. Chem. Phys.* **2003**, *118*, 487.
(20) Barone, V.; Cossi, M. *J. Phys. Chem. A* **1998**, *102*, 1995.
(21) Jaussaud, C. Ph.D. Thesis, Université Paris Sud, Orsay, France, 2003.
(22) Buzko, V. Y.; Polushin, A. A.; Sukhno, I.V. *Aqueous Solutions*, version 1.2; Kuban State University: Krasnodar, Russia, 2004; adapted in English by Pettit, D. L. Academic Software: United Kingdom; available at www.acadsoft.co.uk.
(23) Topin, S.; Aupiais, J.; Baglan, N.; Vercouter, T.; Vitorge, P.; Moisy, P. *Anal. Chem.* **2009**, *81*, 5354.

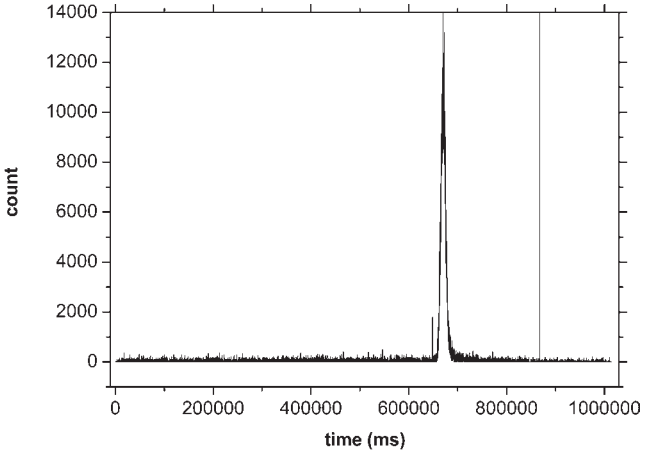


**Figure 1.** Electropherogram of a Pa(V) $\sim 10^{-7}$ M in 0.5 M oxalic acid. The vertical line corresponds to the position related to the bulk electrolyte velocity. At its right side all species are under cationic form, at its left side they are anionic.

To determine more accurately the charge of the complex, experiments were conducted with Np(V) and U(VI) under the same experimental conditions. The corresponding electropherogram is represented in Figure 2 in terms of mobility. U(VI) oxalate complex mobility ($-3.02 \times 10^{-4}$ cm$^2$ V$^{-1}$ s$^{-1}$) is significantly lower than that of Np(V) and Pa(V) oxalate complexes ($-3.67$ and $-3.93 \times 10^{-4}$ cm$^2$ V$^{-1}$ s$^{-1}$ respectively), the error associated to mobility values lying between 3 and 5%. The more charged species is expected to display the higher mobility. However, according to literature, $UO_2(C_2O_4)_3^{4-}$ and $NpO_2(C_2O_4)_2^{3-}$ are the oxalate complexes of maximum order for U(VI) and Np(V) in acidic medium.[24] Mixed hydroxo oxalato complexes of Np(V) have been observed but at pH higher than 9.[24] For Pa(V), results of solvent extraction experiments described in part 2.1, allow to exclude the presence of hydroxyl group in the complex of maximum order. The inversion in Figure 2 has already been observed in the case of complexes that bear charges higher than 3, like carbonate complexes of lanthanides.[25] The charge of the highly anionic complex $UO_2(C_2O_4)_3^{4-}$ should be compensated by ion pairing between protons and this complex, this phenomenon being favored by the acidity used in this work. Similar mobilities (within error bars) observed for Np(V) and Pa(V) oxalate complexes lead to the conclusion that the charge of the Pa(V) complex is $-3$. The small difference can be related to a difference in size of both complexes. Possible complexes are therefore $PaO(C_2O_4)_3^{3-}$ and $Pa(C_2O_4)_4^{3-}$.

**1.2. XAS Experiments.** To ascertain the presence or absence of a mono oxo bond of aqueous protactinium oxalate, XAS experiments were performed on two samples, both containing oxalic acid at high concentration (1 and 0.8 M) with a ratio $C_{ox}/C_{Pa}$ of around 80 and 160, respectively (formation of the limiting complex). The Pa $L_{III}$ edge

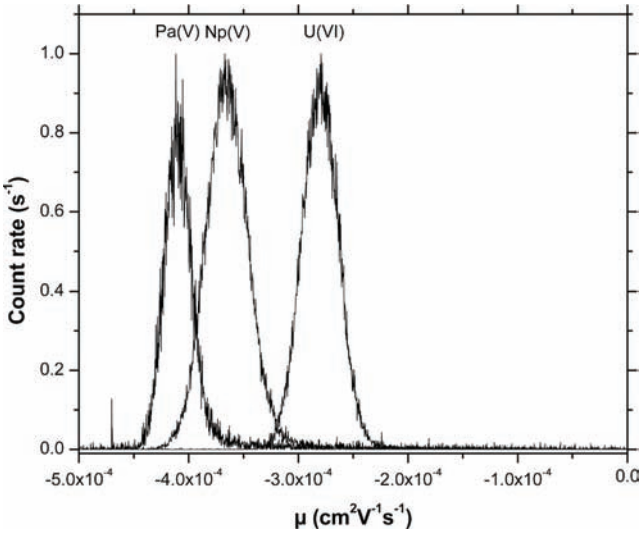


**Figure 2.** Comparison between electrophoretic mobilities of Pa(V), Np(V) and U(VI) oxalate complexes under the same experimental conditions as in Figure 1.

XANES spectra of the two solutions do not exhibit the characteristic multiple scattering shoulder at roughly 15 eV above the edge maximum (Supporting Information, Figure S1). This absence indicates that protactinium does not form a transdioxo bond in these conditions as already observed in 0.5 M hydrofluoric acid.[4,17] However, it does not preclude the occurrence of a monooxo bond as in the case of 13 M sulfuric acid.[3,4] Figures 3a and 3b show the Pa $L_{III}$ edge EXAFS spectra and the associated modulus of the Fourier transform (FT) obtained for the 1.0 M oxalic acid solution. Similar spectra (not shown) have been observed on the 0.8 M sample.

In Figure 3b peak A corresponds to a short Pa-ligand contribution which can be attributed to a Pa-oxo bond. Since the XANES spectrum indicates the absence of a transdioxo bond, the number of oxo ligand has been fixed to one in the data fit, as already observed in concentrated sulfuric acid.[4] Peak B and D, at R+$\phi$ of 1.9 and 3.7 Å, respectively (not phase corrected), indicates the presence of oxalate ligands with oxygen atoms linked to Pa and the corresponding number of distal (more distant) oxygen atoms. The oxalate ligand can coordinate either in side-on or end-on mode as depicted in Figure 4. These two coordination modes show different interatomic distances which can be used to interpret the actual ligand arrangement.

Crystal structure data of protactinium oxalates are not available so far. Instead we noted in the coordination scheme typical interatomic distances of U(VI) oxalates because the ionic radii of Pa(V) and U(VI) (eight-coordinate) are similar (Pa(V) = 1.05 Å, U(VI) = 1.0 Å). Although the first metal−oxygen distance comprises a wide range of values, the average value of the side-on coordination (2.42 Å) is significantly shorter than that of the end-on arrangement (2.58 Å).[26−30] There is also a significant difference in metal−carbon distances. The linear arrangement of two carbon atoms in the end-on arrangement would result in a strong multiscattering signal, as has been observed for example in case of U(IV) carbonate for the linear arranged C−O bonds.[31] However,

(24) Hummel, W.; Anderegg, G.; Rao, L.; Puigdomènech, I.; Tochiyama, O. *Chemical Thermodynamics of Coumpounds and Complexes of U, Np, Pu, Am, Tc, Se, Ni and Zr with Selected Organic Ligand*; Monpean, F. J., Illemassène, M., Perrone, J., Eds.; Elsevier: Amsterdam, 2005.
(25) Philippini, V.; Vercouter, T.; Aupiais, J.; Topin, S.; Ambard, C.; Chaussé, A.; Vitorge, P. *Electrophoresis* **2008**, *29*, 2041.
(26) Alcock, N. W. *J. Chem. Soc.* **1973**, *16*, 1610.
(27) Alcock, N. W. *J. Chem. Soc.* **1973**, *16*, 1616.
(28) Legros, J. P.; Jeannin, Y. *Acta Crystallogr., Sect. B* **1976**, *32*, 2497.
(29) Szabó, Z.; Fisher, A. *Acta Crystallogr., Sect. E* **2002**, *58*, 56.
(30) Giesting, P. A.; Porter, N. J.; Burns, P. C. *Z. Kristallogr.* **2006**, *221*, 252.
(31) Hennig, C.; Ikeda-Ohno, A.; Emmerling, F.; Kraus, W.; Bernhard, G. *Dalton Trans.* **2010**, *39*, 3744.

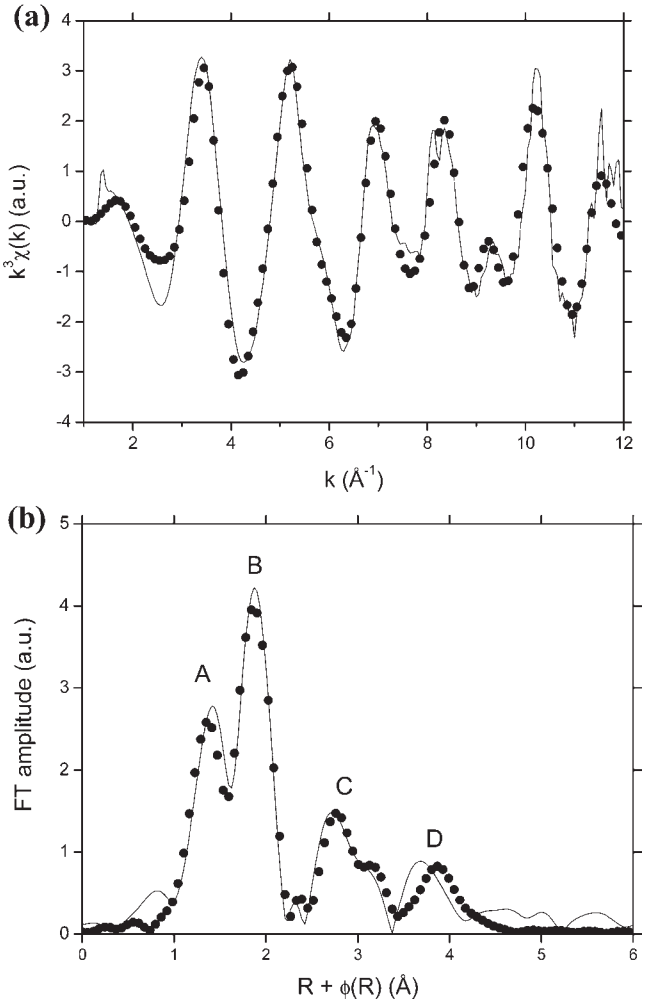


**Figure 3.** (a) Experimental (straight line) and fitted (dotted line) EXAFS spectra of Pa(V) in 1.0 M $H_2C_2O_4$ solution. (b) Experimental (straight line) and fitted (dotted line) moduli of the FT of Pa(V) in 1.0 M $H_2C_2O_4$.

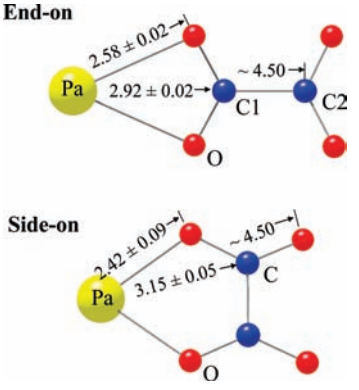


**Figure 4.** Coordination scheme of oxalate in end-on and side-on arrangement. Average interatomic distances with distance variations are taken from crystal structures of U(VI) oxalates.[26−30].

this distance is expected to be similar to the one of ~4.5 Å between Pa and the distal oxygen in side-on mode. Therefore, the coordination will be analyzed here by using the first Pa−O and Pa−C distances.

Table 1 gives the best fit results of EXAFS parameters obtained from this phenomenological description of the protactinium coordination sphere for the two samples. Both, the short Pa−O distance of 2.38 Å as well as the long Pa−C distance of 3.28 Å indicate a side-on coordination of oxalate. In the fit, multiple scattering paths have been taken into account, in particular the triple scattering path of both carbon atoms from each oxalate (Pa−O−C), and the triple and quadruple scattering path of both distal oxygen atoms of each oxalate (Pa−C−$O_{distal}$). The fit does not preclude the presence of an additional water molecule in the first coordination sphere as coordination numbers are in the order of 15% of the determined values. A difference of one unit in the first coordination sphere (resulting in 14% difference) would therefore not affect the fit but only slightly the Debye−Waller factor. Finally no further peak is observed in the modulus of the FT above 5 Å, indicating that oxalate complexation prevents polymerization under the experimental conditions used here.

EXAFS measurements have been performed by Vallet et al. on $UO_2(C_2O_4)_3^{4-}$ in aqueous solution.[32] The reported uranium-oxalate oxygen bond distance (2.37 Å) is remarkably similar to the one determined in the present work for protactinium. Same observation concerning the cation-oxalate carbon bond distance (3.26 Å) can be made. The authors concluded that two bidentate oxalates and a third unidentate oxalate are bonded to the uranyl cation because the transdioxo cation $UO_2^{2+}$ unit restricts the coordination exclusively to the equatorial plane and the experimental determined coordination number of the equatorial plane was determined to be 5. In contrast, the one oxo atom of the monooxo cation $PaO^{3+}$ unit restricts the coordination only to one hemisphere, and therefore, three oxalate ions are able to coordinate in side-on arrangement

**1.3. .Quantum Chemical Calculations.** Because EXAFS provides only a radial distribution function of the back-scattering atoms, DFT calculations were performed to optimize the spatial ligand arrangement of the $PaO(C_2O_4)_3^{3-}$ complex. Geometrical parameters at the RECP/B3LYP and RECP/PBE0 levels, in vacuum condition and in solution, are presented in Table 2. The so optimized structure is presented in Figure 5.

Distances given by EXAFS data and DFT are in a good agreement. Maximum deviations between EXAFS data and calculations of 1.3% for the Pa−O distance at 2.38 Å, 0.9% for the Pa−C distance, and 0.7% for the Pa−$O_{distal}$ are obtained. The oxygen atoms of carboxylates in the first coordination sphere of protactinium in the complex $PaO(C_2O_4)_3^{3-}$ are arranged like water molecules' oxygen in $PaO(H_2O)_6^{3+}$.[17] However, quantum chemical calculations show a significantly longer Pa−$O_{oxo}$ distance than that observed by EXAFS. A similar phenomenon has already been observed in other works with protactinium but not with uranium(VI).[17,33]

The results obtained by using two experimental techniques coupled with theoretical calculations are in good agreement with each other. According to the EXAFS data and DFT calculations, $PaO^{3+}$ is surrounded by 3 bidentate oxalates in side-on arrangement. The charge of this complex has been deduced to be −3 from CE-ICP-MS measurements. Since the presence of a hydroxyl group can be excluded according to solvent extraction

(32) Vallet, V.; Moll, H.; Wahlgren, U.; Szabó, Z.; Grenthe, I. *Inorg. Chem.* **2003**, *42*, 1982.
(33) Siboulet, B.; Mardsen, C. J.; Vitorge, P. *New J. Chem.* **2008**, *32*, 2080.

**Table 1.** EXAFS Best Fit Parameters Obtained for the Two Solutions at the Pa $L_{III}$ Edge[a]

| $C_{H2C2O4}$ | A | B | C, D | |
|---|---|---|---|---|
| 1 M | | | **6.1** C at 3.28(1) Å<br>$\sigma^2$ = 0.0019 Å$^2$ | $S_0^2$ = 0.7<br>$\Delta e_0$ = 4.53 eV |
| | *1* $O_{oxo}$ at 1.75(1) Å<br>$\sigma^2$ = 0.0027 Å$^2$ | **6.1** $O_{oxalate}$ at 2.38(1) Å<br>$\sigma^2$ = 0.0065 Å$^2$ | $\sigma_3^2$ = 0.0060 Å$^2$ | $\varepsilon$ = 0.0055 |
| | | | **6.1** O at 4.47(5) Å<br>$\sigma^2$ = 0.0417 Å$^2$ | $r$ = 4.4%<br>$CHI^2_r$ = 0.1 |
| 0.8 M | *1* $O_{oxo}$ at 1.73(1) Å<br>$\sigma^2$ = 0.0051 Å$^2$ | **6.3** $O_{oxalate}$ at 2.37(1) Å<br>$\sigma^2$ = 0.0067 Å$^2$ | **6.3** C at 3.27(1) Å<br>$\sigma^2$ = 0.0030 Å$^2$ | $S_0^2$ = 0.8<br>$\Delta e_0$ = 4.67 eV |
| | | | **6.3** O at 4.44(3) Å<br>$\sigma^2$ = 0.0369 Å$^2$ | $\varepsilon$ = 0.0056<br>$r$ = 3.2%<br>$CHI^2_r$ = 0.1 |

[a] $S_0^2$ is the global amplitude factor, $\Delta e_0$ is the adjusted threshold energy, $\varepsilon$ is the spectrum noise, $r$ is the $r$-factor of the fit, $CHI^2_r$ is the reduced chi square of the fit. Numbers in italics have been fixed, bold numbers have been linked in the fitting procedure. Errors are given in brackets.

**Table 2.** Geometrical Parameters for the Complex $PaO(C_2O_4)_3^{3-}$ Obtained by Quantum Chemical Calculations Compared to EXAFS Results[a]

| | | B3LYP | | PBE0 | |
|---|---|---|---|---|---|
| distances | EXAFS | vacuum | solution | vacuum | solution |
| Pa−$O_{oxo}$ | 1.75 | 1.89 | 1.90 | 1.87 | 1.88 |
| Pa−$O^x$ ($x$ = 1,2,3,4) | | 2.41 | 2.39 | 2.39 | 2.37 |
| Pa−$O^5$ | | 2.42 | 2.40 | 2.40 | 2.38 |
| Pa−$O^6$ | | 2.30 | 2.28 | 2.28 | 2.26 |
| average Pa−O | 2.38 | 2.39 | 2.37 | 2.37 | 2.35 |
| Pa−$C^x$ ($x$ = 1,2,3,4) | | 3.32 | 3.29 | 3.30 | 3.27 |
| Pa−$C^5$ | | 3.29 | 3.26 | 3.27 | 3.24 |
| Pa−$C^6$ | | 3.24 | 3.21 | 3.21 | 3.18 |
| average Pa−C | 3.28 | 3.30 | 3.27 | 3.28 | 3.25 |
| Pa−$O^x$ ($x$ = 7,8,9,10) | | 4.52 | 4.50 | 4.49 | 4.46 |
| Pa−$O^{11}$ | | 4.50 | 4.47 | 4.47 | 4.44 |
| Pa−$O^{12}$ | | 4.42 | 4.39 | 4.38 | 4.35 |
| average Pa−O | 4.47 | 4.50 | 4.48 | 4.47 | 4.44 |

[a] All distances are in Ångström.

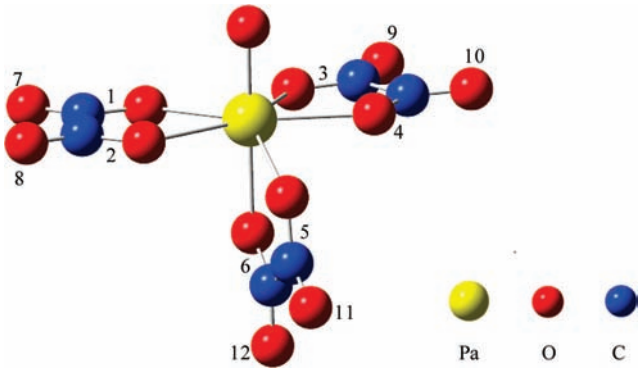


**Figure 5.** Optimized structure of the complex $PaO(C_2O_4)_3^{3-}$ obtained by DFT.

results, the complex of maximum order can be regarded as $PaO(C_2O_4)_3^{3-}$.

**2. Thermodynamics Study.** To avoid the polymerization of protactinium, that is known to occur at concentrations of the element higher than $10^{-5}$ M, the thermodynamic study was performed at tracer scale ($C_{Pa} \sim 10^{-12}$ M).[8] At such low concentration, solvent extraction leads only to differences in the properties of the species present in both phases: the derivation of the mathematical expression of the distribution coefficient $D$ with respect to the equilibrium concentration of extractant or ligand is

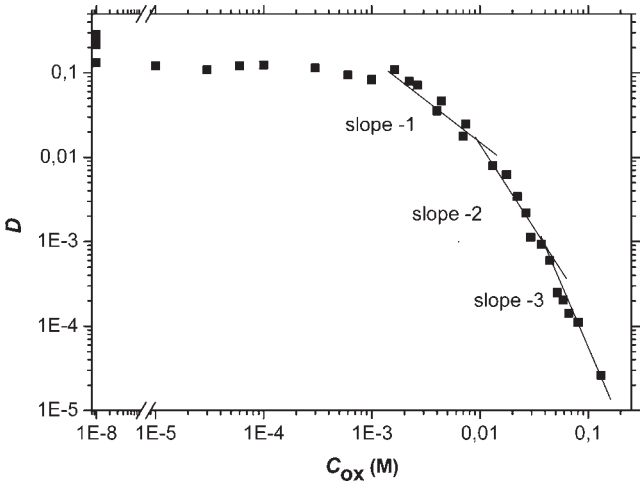


**Figure 6.** Distribution coefficients of Pa(V) as a function of total oxalic acid concentration at $\mu$ = 3 M, $C_{TTA}$ = 0.08 M, $\theta$ = 40 °C, and $[H^+]$ = 0.5 M.

equal to the differences between the mean number of extractant or ligand molecules per metal atom in the complexes present in each phase. The charge of the complexes in aqueous phase is deduced from the derivation of $D$ with respect to proton concentration.[34]

The Pa species involved in the system TTA/toluene/$H_2O$/$NaClO_4$/$HClO_4$/$H_2C_2O_4$ have been characterized in that way.

**2.1. Identification of Complexes.** In Figure 6, the variations of the distribution coefficient $D$ of Pa(V) are plotted as a function of the total oxalic acid concentration ($C_{ox}$). A $D$ value named $D_0$ is obtained in a media without complexing agent and represented arbitrarily at $C_{ox} = 10^{-8}$ M. $D_0$ values are followed by a plateau. The absence of a maximum in the extraction curve indicates that there is no oxalate in the extracted complex.[35] Then, from $C_{ox}$ around $10^{-3}$ M, the decrease in $D$ values can be correlated with the formation of Pa(V) oxalate complexes in aqueous phase.

At constant ionic strength and temperature, the slopes of the logarithmic variations of $D$ with ligand concentration represent the mean number of ligands per Pa atom of the predominant species in aqueous phase. In our experimental

(34) Adloff, J. P.; Guillaumont, R. *Fundamentals of Radiochemistry*; CRC Press: Boca Raton, FL, 1993.

(35) Guillaumont, R.; Muxart, R.; Bouissières, G. Solvent extraction of hydroxo- and acido-complexes in the presence of a chelating agent. The phosphato- and trichloroaceto-complexes of pentavalent protactinium. In *Solvent Extraction Chemistry*; Dyrssen, D., Liljenzin, J. O., Rydberg, J., Eds.; Wiley: New-York, 1967.

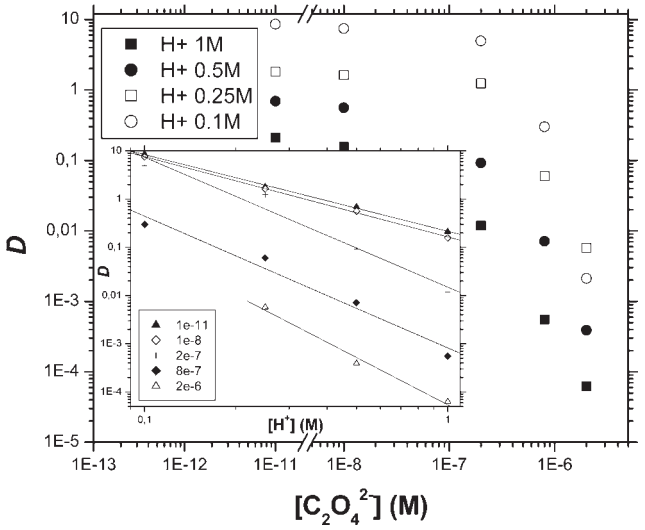


**Figure 7.** Distribution coefficients of Pa(V) as a function of $C_2O_4^{2-}$ concentration at $\mu$ = 3 M, $C_{TTA}$ = 0.08 M and $\theta$ = 25 °C for different values of free proton concentrations. (Inset: Distribution coefficients of Pa(V) as function of proton concentration at $\mu$ = 3 M, $C_{TTA}$ = 0.08 M and $\theta$ = 25 °C for different concentrations of $C_2O_4^{2-}$ represented with the linear adjustments).

conditions, three Pa(V) oxalate complexes are formed successively. According to XAS and CE-ICP-MS results the number of oxalate ligands is limited to three. With the same technique, Guillaumont observed only two oxalate complexes of protactinium, at a constant ionic strength $\mu$ = 3 M, $C_{TTA}$ = 0.1 M whatever the acidity between 1 and 3 M.[8] This difference in the number of oxalate complexes of protactinium observed in the aqueous phase can be related to the difference in the oxalate concentration used. In Guillaumont's work, the total oxalic concentration does not exceed $2 \times 10^{-2}$ M, a value that corresponds to the beginning of the formation of the third complex in our experimental conditions (Figure 6).

A maximum order of three has been observed with $U^{VI}O_2^{2+}$ oxalates using potentiometry and spectrophotometry whereas only two complexes were deduced from solvent extraction experiments under the same experimental conditions ($\mu$ = 3 M $NaClO_4$ and $\theta$ = 25 °C).[24] With the same technique, $Np^{V}O_2^{+}$ was proved to form two complexes or even only one respectively in NaCl and $NaClO_4$ (3 *m*, 25 °C).[24] Oxalate complexation of $Pu^{4+}$ is more controversial: four oxalate complexes were identified through solubility experiments at 1 M $HNO_3$ whereas only two and three complexes were observed using solvent extraction respectively in 4 M ($HNO_3 + NaNO_3$) and 1 M $HClO_4$.[24]

The mean charge of the predominant species in the aqueous phase has been deduced from the variations of *D* values as a function of $C_2O_4^{2-}$ concentration for different free proton concentration varying from 0.1 to 1 M as illustrated in Figure 7. The distribution coefficient of Pa(V) decreases with the increase in acidity leading to a difference of about 2 orders of magnitude in *D* values between the lower and the upper proton concentrations.

For given values of free ligand concentration, the logarithmic variations of *D* as a function of $[H^+]$ are linear allowing the calculation of the mean charge of the complexes in aqueous phase through the determination of the mean number of hydroxide present in the complexes (inset in Figure 7).[34] In the oxalate concentration range corresponding to the plateau, a number of hydroxide close to 1 was observed leading to the predominance of the first hydrolysis species of Pa(V) ($PaO(OH)^{2+}$). At higher oxalate concentration, a number of hydroxide groups close to 0 is obtained. According to the structural study, the mono oxo bond is observed in the complex of higher order. Therefore, the mono oxo bond has been assumed to be present in the complexes of lower order. This leads to the conclusion that the predominant species are successively: $PaO(C_2O_4)^{+}$, $PaO(C_2O_4)_2^{-}$, and $PaO(C_2O_4)_3^{3-}$.

A mean value of 4.1 ± 0.7 molecules of TTA per Pa atom in the extracted species was determined for oxalic acid concentration lower than $3 \times 10^{-2}$ M when varying the chelatant concentration from 0.05 to 0.08 M (Supporting Information, Figures S2 to S5). In our experimental conditions ($[H^+]$ = 0.5 M) the first hydrolyzed species of Pa(V) is present in solution. Since no ligands are present in the extracted neutral chelate, the protactinium species in the organic phase must be $PaO(OH)(TTA)_2(HTTA)_2$. Neutralization of Pa(V) cation occurs via TTA bidentate molecules, and the coordination is completed with two undissociated HTTA, leading to the formation of self-adducts.[36] That result is in good agreement with the value of 4 TTA molecules per Pa atom determined by Guillaumont in the TTA concentration range of 0.03 to 0.5 M (in $\mu$ = 3 M, $[H^+]$ = 3 M, and $C_{ox} = 6 \times 10^{-3}$ M).[8]

**2.2. Determination of Formation Constants and Thermodynamic Data.** The initial form of Pa(V) involved in the formation of oxalate complexes has been assumed to be $PaO(OH)^{2+}$, the predominant species in absence of ligand ($[H^+]$ = 0.5 M).[5,37] Therefore, chemical equilibria under study are written

$$PaO(OH)^{2+} + iC_2O_4^{2-} + H^{+} \overset{\beta_{app,i}}{\rightleftharpoons} PaO(C_2O_4)_i^{(3-2i)+} + H_2O \quad \text{with} \quad \beta_{app,i} = \frac{[PaO(C_2O_4)_i^{(3-2i)+}]}{[PaO(OH)^{2+}][C_2O_4^{2-}]^i[H^+]} \tag{3}$$

$$Pa(V) + iOx \overset{\beta_{cond,i}}{\rightleftharpoons} Pa^{V}(Ox)_i \quad \text{with} \quad \beta_{cond,i} = \frac{[Pa^{V}(Ox)_i]}{[Pa(V)][Ox]^i} \tag{4}$$

Where Ox is oxalic acid (whatever its chemical forms), and $\beta_{app}$ and $\beta_{cond}$ are apparent and conditional formation constants, respectively. Both the apparent and conditional formation constants are written in terms of concentration instead of activities. Working at constant ionic strength and temperature ensure that activity coefficients are constant throughout solvent extraction experiments. Apparent and conditional constants are

(36) Rydberg, J.; Sekine, T. *Principles and Practices of Solvent Extraction*; Rydberg, J., Musikas, C., Choppin, G. R., Eds.; Marcel Dekker: New York, 1992.
(37) Trubert, D.; Le Naour, C.; Jaussaud, C. *J. Sol. Chem.* **2002**, *31*, 261.

**Table 3.** Equilibrium Constants and Standard Enthalpy Variations Relative to Successive Dissociation of Oxalic Acid

| $\log K^0_{a_1}$ | $\log K^0_{a_2}$ | $\Delta H^0_1$ (kJ mol$^{-1}$) | $\Delta H^0_2$ (kJ mol$^{-1}$) |
|---|---|---|---|
| $-1.40 \pm 0.03$ | $-4.25 \pm 0.01$ | $-3.3 \pm 0.5$ | $-7.3 \pm 0.1$ |

related according to:

$$\beta_{app} = \alpha \times \beta_{cond} \quad (5)$$

Where

$$\alpha = 1 + 10^{pK_{a_1}}[H^+] + 10^{pK_{a_1} \times pK_{a_2}}[H^+]^2 \quad (6)$$

In eq 6, the values $pK_{a_1}$ and $pK_{a_2}$ are the dissociation constants of oxalic acid related to the following equilibria:

$$H_2C_2O_4 \overset{K_{a1}}{\rightleftarrows} HC_2O_4^- + H^+ \quad (7)$$

$$HC_2O_4^- \overset{K_{a2}}{\rightleftarrows} C_2O_4^{2-} + H^+ \quad (8)$$

Thermodynamic data concerning successive dissociations of oxalic acid at infinite dilution and 298.15 K taken from literature are listed in Table 3.[24]

They were adjusted to our experimental temperature (eq 9) and ionic strength using the SIT methodology (eq 10 and 11).[38]

$$\log K^0(T) = \log K^0(T_0) + \frac{\Delta H^0(T_0)}{R \ln 10} \times \left(\frac{1}{T_0} - \frac{1}{T}\right) \quad (9)$$

$$\log K_{a_1} + 2D_{DH} - \varepsilon(H^+, ClO_4^-) \times m_{ClO_4^-} = \log K^0_{a_1} - \Delta\varepsilon_1(Na^+) \times m_{Na^+} \quad (10)$$

$$\log K_{a_2} + 4D_{DH} - \varepsilon(H^+, ClO_4^-) \times m_{ClO_4^-} = \log K^0_{a_2} - \Delta\varepsilon_2(Na^+) \times m_{Na^+} \quad (11)$$

$$D_{DH} = \frac{A\sqrt{I_m}}{1 + Ba\sqrt{I_m}} \quad (12)$$

Where $D_{DH}$ is the Debye−Hückel coefficient, $m_{ClO_4^-}$ and $m_{Na^+}$ are the molality of $ClO_4^-$ and $Na^+$, respectively, and the SIT interaction parameters are $\Delta\varepsilon_1(Na^+) = -\varepsilon(Na^+, HC_2O_4^-)$ and $\Delta\varepsilon_2(Na^+) = \varepsilon(Na^+, HC_2O_4^-) - \varepsilon(Na^+, C_2O_4^{2-})$. For the calculation of $pK_{a_1}$ and $pK_{a_2}$ at temperatures other than 25 °C, the SIT parameters $\varepsilon$ were assumed to be independent of temperature, and the values available at 25 °C were used.[24] The temperature dependence of the parameters $A$ and $B$ involved in the Debye−Hückel coefficient, $D_{DH}$, was taken into account whereas the parameter, $a$, related to the size of the hydrated ion, was assumed independent of temperature.[38]

(38) Allard, B.; Banwart, S. A.; Bruno, J.; Ephraim, J. H.; Grauer, R.; Grenthe, I.; Hadermann, J.; Hummel, W.; Jakob, A.; Karapiperis, T.; Plyasunov, A. V.; Puigdomènech, I.; Rard, J. A.; Saxena, S.; Spahiu, K. *Modelling in Aquatic Chemistry*; OCDE: Paris, France, 1997.

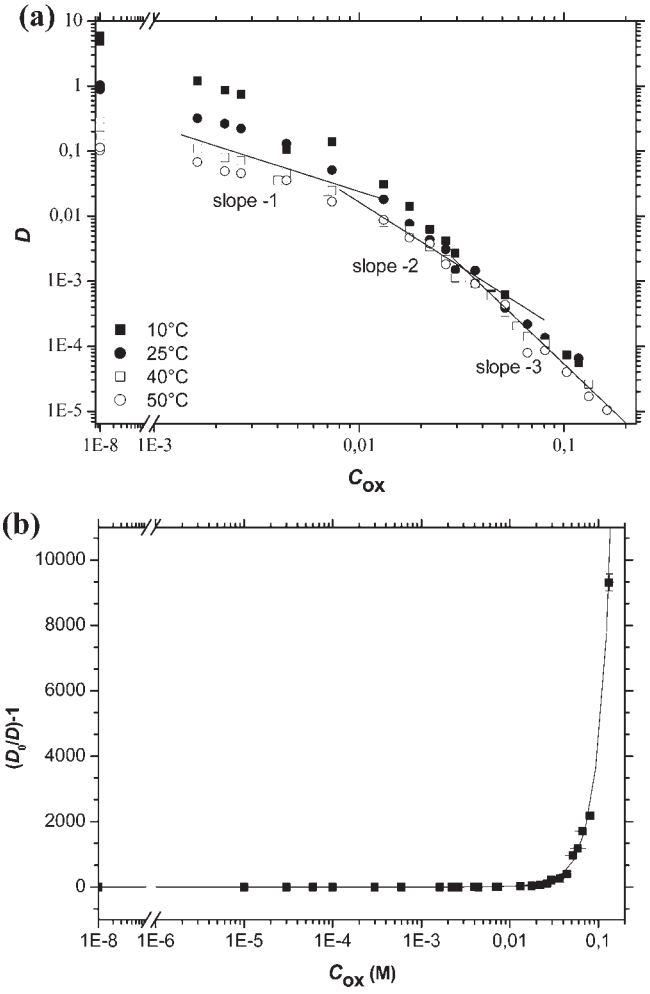


**Figure 8.** (a) Distribution coefficients of Pa(V) as function of total oxalic acid concentration at $\mu = 3$ M, $C_{TTA} = 0.08$ M, and $[H^+] = 0.5$ M for different values of temperature. (b) Fit example: $((D_0/D) - 1)$ as a function of total oxalic acid concentration at $\mu = 3$ M, $\theta = 40$ °C, $[H^+] = 0.5$ M, and $C_{TTA} = 0.08$ M.

**Table 4.** Dissociation Constants of Oxalic Acid at $\mu = 3$ M for Different Values of Temperature

| | temperature (K) | | | |
|---|---|---|---|---|
| | 283.15 | 298.15 | 313.15 | 323.15 |
| $pK_{a_1}$ | $1.15 \pm 0.03$ | $1.16 \pm 0.03$ | $1.19 \pm 0.03$ | $1.20 \pm 0.03$ |
| $pK_{a_2}$ | $3.64 \pm 0.01$ | $3.68 \pm 0.01$ | $3.73 \pm 0.01$ | $3.76 \pm 0.01$ |

For each value of temperature, the raw extraction data $((D_0/D) - 1)$, listed in Supporting Information, Table S1, were plotted as function of the total oxalic acid concentration and adjusted with a polynomial of third order taking into account experimental errors on $D$ values and oxalic acid concentration. The error on the oxalic acid content was set as equal to 10% of the concentration. The error on $((D_0/D) - 1)$ includes the error on the determination of $D_0$ as same as the error coming from $D$ values.

Subsequently, the coefficients of this polynomial were converted into apparent formation constants using the values of $K_{a_1}$ and $K_{a_2}$ with their associated errors (eq 13).

$$\frac{D_0}{D} - 1 = \sum_{i=1}^{3} \beta_{app,i}[C_2O_4^{2-}]^i \quad (13)$$

**Table 5.** Apparent Formation Constants of Oxalate Complexes of Protactinium[a]

| | this work | | | | 8 | 2 |
|---|---|---|---|---|---|---|
| | $\mu$ = 3 M, [H$^+$] = 0.5 M | | | | $\mu$ = 3 M, 1 M ≤ [H$^+$] ≤ 3 M | $\mu$ = 3 M, $10^{-3}$ M ≤ [H$^+$] ≤ 3 M |
| $\theta$ (°C) | 10 | 25 | 40 | 50 | 25 | 25 |
| log $\beta_{app,1}$ | 7.6 ± 0.2 | 7.4 ± 0.3 | 7.5 ± 0.3 | 7.1 ± 0.1 | 7.0 | 7.1 |
| log $\beta_{app,2}$ | 14.8 ± 0.6 | 14.5 ± 0.8 | 13.8 ± 0.5 | 13.6 ± 0.8 | 14.4 | 14.0 |
| log $\beta_{app,3}$ | 20.4 ± 0.4 | 19.1 ± 0.7 | 19.6 ± 0.4 | 19.5 ± 0.3 | | 19.0 |

[a] The assigned uncertainties represent 2$\sigma$.

The variations of $D$ versus $C_{ox}$ presented in Figure 8a indicate a decrease in $D$ values when the temperature increases. This effect is much less pronounced than that observed in sulfate media.[3] The variations of $((D_0/D) - 1)$ and the corresponding adjustment are illustrated in Figure 8b for $\theta = 50$ °C.

The procedure was repeated for each temperature value, leading to a set of apparent formation constants $\beta_{app,i}$ that are listed in Table 5 together with the few data available in the literature.

The formation constants reported by Guillaumont and Carrère are originally related to non dissociated oxalic acid.[2,8] For comparison purpose, their constants were adjusted using the acidity constants listed in Table 4. The so obtained formation constants are in fair agreement with the ones determined in the present work (Table 5).

Comparing values of formation constants of oxalate complexation of Np(V) (log $\beta_{app,1}$ = 3.61 ± 0.2 at 3 *m* $NaClO_4$ and log $\beta_{app,2}$ = 7.07 ± 0.15 at 3 *m* NaCl) shows that Pa(V) ($PaO^{3+}$) complexation can not be compared with one of Np(V) ($NpO_2^+$).[24] Oxalate complexation of $U^{VI}O_2^{2+}$ has been studied with spectrophotometric, potentiometric, and solvent extraction methods. Similar results obtained at 3 M $NaClO_4$ and 25 °C, leads to stability constants log $\beta_{app,1}$ = 6.2 ± 0.2, log $\beta_{app,2}$ = 11.3 ± 0.2, and log $\beta_{app,3}$ = 14.5 ± 0.7.[24]

First, the stepwise formation constants $K_i$ (related to $\beta_i = \prod K_i$) can give information on the type of coordination.[24] The stability constants of oxalate complexes of Pa follow the sequence $K_1 > K_2 > K_3$ whatever the temperature value during the experiment. The ratio $K_1/K_2$ and $K_2/K_3$ vary between 2.3 and 14.9, 2.8, and 283.1 respectively, as the temperature increases. These values are much higher than the theoretical ones relative to a six, seven, and eight-fold coordinated cation and based on pure statistical effects involving a displacement of a water molecule by a ligand.[36] Obviously, other effects such as electrostatic, geometric, and chelate formation influence the complexation of Pa with oxalate.

Similarities in the order of magnitude of stepwise formation constants are commonly correlated with a similar coordination of each ligand. Although the coordination mode of the third oxalate in $UO_2(C_2O_4)_3^{4-}$ remains controversial, it has been proven that the first two oxalates are coordinated to uranium in the side-on mode.[24] Stepwise formation constants of the three Pa(V) oxalate complexes determined in that study have the same order of magnitude than the first two $K_i$ of $UO_2^{2+}$ oxalate complexes.[24,39,40] The coordination mode of the oxalates in Pa(V) oxalate complexes can therefore be assumed to be identical to the one observed in the first two U(VI) oxalate complexes: the bidendate side-on mode.

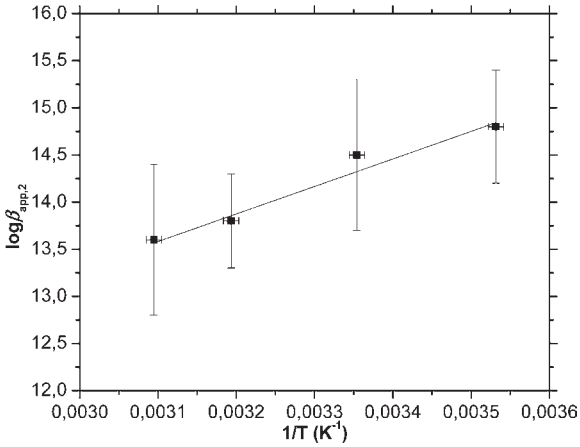


**Figure 9.** Variation of log $\beta_{app,2}$ as function of temperature at $\mu$ = 3 M.

Temperature dependence of the apparent formation constants of oxalate complexes of Pa(V) was analyzed using the Van't Hoff's equation, neglecting the variation of enthalpy with temperature ($\Delta C_p = 0$). This leads to the reduced eq 14:[41]

$$\log \beta = -\frac{\Delta H(T_0)}{R \ln 10} \cdot \frac{1}{T} + \frac{\Delta S(T_0)}{R \ln 10} \qquad (14)$$

where $R$ is the gas constant and $T_0$ the reference temperature.

The variations of log $\beta_{app,2}$ as function of $1/T$ are illustrated in Figure 9.

$\Delta G$ values listed in Table 6 indicate very stable oxalate complexes of protactinium which stability increases with the order of the complex. All reactions of formation of these complexes are strongly exothermic and coupled with an entropic contribution that increases with the number of ligands. That strong entropic variation matches with the oxalate coordination mode of protactinium. The switch of a mono coordinate water molecule by a bidentate oxalate leads to the release of two $H_2O$ molecules and therefore, an increase of disorder. Considering the stepwise complexation equilibria characterized by the constants $K_{app,1}$, $K_{app,2}$, and $K_{app,3}$ allows to bypass the contribution of dehydration of the oxalate ligand to the thermodynamic parameters

(39) Ferri, D.; Iuliano, M.; Manfredi, C.; Vasca, E.; Caruso, T.; Clemente, M.; Fontanella, C. *Dalton Trans.* **2000**, 3460.
(40) Di Bernardo, P.; Zanonato, P. L.; Tian, G.; Tolazzi, M.; Rao, L. *Dalton Trans.* **2009**, *23*, 4450.
(41) Puigdomènech, I.; Rard, J. A.; Plyasunov, A. V.; Grenthe, I. *TDB−4. Temperature corrections to thermodynamic data and enthalpy calculations*; OCDE: Issy-les-Moulineaux, France, 1999.

**Table 6.** Thermodynamic Data Related to the Formation Equilibria of Oxalate Complexes of Protactinium at 25 °C

| | $\Delta G$ (kJ mol$^{-1}$) | $\Delta H$ (kJ mol$^{-1}$) | $\Delta S$ (J.mol$^{-1}$.K$^{-1}$) | $T\Delta S$ (kJ mol$^{-1}$) |
|---|---|---|---|---|
| $\beta_{app,1}$ | $-42 \pm 6$ | $-22 \pm 6$ | $69 \pm 21$ | $21 \pm 7$ |
| $\beta_{app,2}$ | $-82 \pm 7$ | $-56 \pm 7$ | $87 \pm 23$ | $26 \pm 7$ |
| $\beta_{app,3}$ | $-114 \pm 19$ | $-35 \pm 19$ | $263 \pm 63$ | $78 \pm 18$ |

since it can be assumed to be the same for the three equilibria. The corresponding enthalpy variations deduced from Table 6 indicate that the first two complexation reactions are still endothermic whereas the third one becomes exothermic ($\Delta H(K_{app,3}) = 21 \pm 26$ kJ mol$^{-1}$). The entropy variation relative to the formation of the complex (1,2) ($18 \pm 44$ J·mol$^{-1}$.K$^{-1}$) becomes much lower than that of the first and the third complexes. One could notice that the formation of the complex (1,2) involves a transition from a cationic species to an anionic one. The entropic gain associated to the disruption of the hydration sphere around the initial species, is likely to be counterbalanced by a loss of entropy because of the new ordering of charges around the formed complex. The entropy variation associated to the third complex ($\Delta S(K_{app,3}) = 176 \pm 86$ J·mol$^{-1}$.K$^{-1}$) is unexpectedly high: there is no more balancing between disruption and ordering. The gain due to the release of water molecules from the complex (1,2) and perhaps to the loss of symmetry in the complex is much higher than the entropic loss because of the combination between the ions. The unfavorable enthalpy indicates that the energy spent in the dehydration step is not regained in the formation of the third complex.

Only scarce thermodynamic data relative to oxalate complexation of actinides are available in the literature. Results of this work are in agreement with the ones concerning the complexation reactions of U(VI) with oxalate in 1.05 *m* $NaClO_4$, that are proved to be exothermic with high positive entropic variations.[40,42] Moreover, complexation implies several processes like dehydration of reagents, bond breaking, and bond formation that are characterized by their own energetic contribution. Furthermore, the lack of data in the literature does not allow to correlate thermodynamic parameters to the structure, especially when the involved cation is molecular.

(42) Kirishima, A.; Onishi, Y.; Sato, N.; Tochiyama, O. *Radiochim. Acta* **2008**, *96*, 581.

## Conclusion

XAS experiments on Pa(V) in oxalic acid revealed the presence of one single Pa−O oxo bond in the complex of maximum order. In that way, the protactinium oxalate complex is similar to the one previously observed in concentrated sulfuric acid. In oxalate media, the monooxo cation $PaO^{3+}$ is surrounded by 3 bidendate oxalate ligands, coordinated in the "side on" bidentate mode as confirmed by DFT calculations. The presence of water molecule in the first coordination sphere can not be completely ruled out. The XAS results agree well with the existence of a highly charged anionic complex deduced from capillary electrophoresis coupled with ICP-MS. To bypass the strong tendency of Pa(V) toward polymerization, the thermodynamic study of oxalate complexation of Pa(V) was performed also at tracer scale using solvent extraction. This systematic study allowed to identify the three oxalate complexes: $PaO(C_2O_4)^+$, $PaO(C_2O_4)_2^-$, and $PaO(C_2O_4)_3^{3-}$, and to determine their formation constants. The stability of the complexes increases with their order. Moreover, the temperature dependence of the cumulative constants was characteristic of exothermic reactions, coupled with a strong positive entropic contribution.

**Acknowledgment.** This work was supported by PACEN/GNR PARIS (French Organization) and ACTINET (European Network). The authors greatly acknowledge Marc Lecomte (CEA-LABRA) for providing the thorium irradiation at the Osiris reactor of CEA Saclay (France). A generous allotment of CPU time on GRIF (http://www.grif.fr) is also gratefully acknowledged.

**Supporting Information Available:** X-ray absorption spectrum of Pa(V) in 1 M oxalic acid at the Pa $L_{III}$ edge and Logarithmic variations of distribution coefficient $D$ at $[H^+] = 1$ M for different concentrations of TTA as a function of total concentration of oxalic acid and Variations of log $D$ as a function of TTA concentration for $[H^+] = 1$ M, 0.25, and 0.1 M at different oxalic acid concentrations, and Values of $D$ and $D_0$. This material is available free of charge via the Internet at http://pubs.acs.org.